Biochimica et Biophysica Acta 1850 (2015) 813–823

Contents lists available at ScienceDirect

Biochimica et Biophysica Acta

journal homepage: www.elsevier.com/locate/bbagen

Mechanisms of protection against diabetes-induced impairment of endothelium-dependent vasorelaxation by Tanshinone IIA

Yan-Hua Li [a,1], Qiang Xu [a,1], Wen-Huan Xu [b], Xin-Hong Guo [a], Shu Zhang [c,*], Yun-Dai Chen [a,**]

[a] Department of Cardiology, PLA General Hospital, Beijing, China
[b] Scientific Research Department, Medical Administrative Division, PLA General Hospital, Beijing, China
[c] Department of Respiration, PLA General Hospital, Beijing, China

ARTICLE INFO

Article history:
Received 11 September 2014
Received in revised form 6 December 2014
Accepted 12 January 2015
Available online 19 January 2015

Keywords:
Tanshinone IIA
Human umbilical vein endothelial cell
Diabetes
High glucose
NO synthase
Phosphorylation

ABSTRACT

Background: Impairment of endothelium-dependent vasorelaxation has been suggested to play a principle role of endothelial dysfunction in the development of cardiovascular complications of diabetes. Recent studies have demonstrated a protective effect of Tanshinone IIA (Tan) on endothelial nitric oxide synthase (eNOS)–NO pathway. However, its role in endothelium-dependent vasorelaxation in diabetes and precise mechanisms remain elusive.

Methods: Sprague–Dawley rats were injected intraperitoneally with streptozotocin (STZ) to induce diabetes and then administered orally with Tan for 2 weeks. For the in vitro study, human umbilical vein endothelial cells (HUVECs) were co-incubated with Tan and high glucose for 48 h.

Results: eNOS expression and NO generation were significantly decreased in diabetic rats. These decreases were accompanied by an impairment of endothelium-dependent relaxation. Administration of Tan ameliorated the aberrant changes in eNOS expression, NO generation and endothelium-dependent relaxation in diabetic rats. Expectedly, Tan also inhibited high glucose-induced decrease of eNOS expression and NO generation in a concentration-dependent manner in HUVECs. Mechanistically, high glucose attenuated eNOS transcriptional activity through inhibiting the binding activity and nuclear translocation of Sp1 and AP-1. However, Tan did not prevent these effects. At post-transcriptional level, Tan increased eNOS expression and activity through multiple mechanisms including regulation of mRNA and protein half-life, degradation, coupling and serine 1177 phosphorylation. Rather than affecting protein phosphatase 2A (PP2A) expression and activity, Tan markedly inhibited the translocation of PP2A-A from cytosol to membrane and subsequently impaired PP2A-A/eNOS interaction, leading to prevent eNOS dephosphorylation. All these alterations underlie the protective role of Tan on eNOS expression following high glucose stimulation.

Conclusions: Our data demonstrate that high glucose decreases eNOS expression initiating at a transcriptional level, whereas Tan prevents such effect through multiple ways of post-transcriptional mechanism.

General significance: Our work provided novel mechanisms for Tan in regulating vasorelaxation and may help to better understand the cardiovascular protective action of Tan.

© 2015 Elsevier B.V. All rights reserved.

1. Introduction

Endothelial cell dysfunction underlies the development of various cardiovascular complications of diabetes [1]. Endothelial nitric oxide synthase (eNOS) is the key enzyme in maintaining vascular endothelium homeostasis. The activity of eNOS is regulated by multiple mechanisms that include transcriptional regulation, post-transcriptional regulation of mRNA stability, and post-translational regulation of protein stability by degradation, reversible coupling and reversible phosphorylation of serine and threonine residues [2,3]. At transcriptional level, although lacking with a typical TATA box, there are a number of transcriptional factors that bind to eNOS promoter, including activator protein-1 (AP-1), Sp1, NF-κB and shear stress-response elements [4,5]. On the other hand, mRNA stability is necessary to maintain eNOS normal expression. In a number of pathological conditions such as inflammation and hypoxia, eNOS mRNA stability is regulated by modulating the binding of some cytoplasmic proteins with eNOS mRNA 3′ untranslated regions (3′-UTR) [3,6]. At post-translational level, phosphorylation of eNOS serine 1179/1177 has been suggested as a central mechanism of

* Correspondence to: S. Zhang, Department of Respiration, PLA General Hospital, No. 28 Fuxing Road, Haidian District, Beijing 100853, China. Tel./fax: +86 66939874.
** Correspondence to: Y.-D. Chen, Department of Cardiology, PLA General Hospital, No. 28, Fuxing Road, Haidian District, Beijing 100853, China. Tel./fax: +86 66939874.
E-mail addresses: zhangshumed@126.com (S. Zhang), chenydmed@126.com (Y.-D. Chen).
[1] These authors contributed equally to this work.

http://dx.doi.org/10.1016/j.bbagen.2015.01.007
0304-4165/© 2015 Elsevier B.V. All rights reserved.

eNOS regulation. Study revealed that serine 1179/1177 of eNOS was distinctively dephosphorylated by protein phosphatase 2A (PP2A), which is a highly conserved and ubiquitous serine/threonine phosphatase [7].

Tanshinone IIA (Tan) is a main active constituent extracted from the rhizome of the *Salvia miltiorrhiza* (Danshen), a traditional Chinese medicinal plant used for preventing and treating cardiovascular disorders [8]. It has functional roles of improving microcirculatory, vasodilatory, anti-thrombotic, anti-inflammatory, free radical scavenging, and mitochondria-protective effects [9,10]. Current research showed that Tan induced vasorelaxation and subsequently reduced blood pressure in hypertension rats, mainly through increasing eNOS expression [11]. On the other hand, it also has been reported that Tan increased eNOS phosphorylation and NO generation in HUVECs [12]. Moreover, Zhou et al. reported that Tan could reverse high glucose-induced eNOS uncoupling, leading to reduce intracellular oxidative stress and increase NO generation [13]. All these findings indicate that Tan plays an important role in maintaining eNOS/NO pathway homeostasis. However, the detailed mechanism by which Tan increases eNOS activity is not well understood, and whether Tan could improve endothelial relaxing dysfunction in diabetes remains enigmatic. In the present study, we investigated the effects of Tan on eNOS expression, NO generation and endothelium-dependent vasorelaxation in diabetic rats.

2. Material and methods

2.1. Materials and reagents

Medium 199 and fetal calf serum were purchased from Gibco (Carlsbad, USA). All other reagents utilized were purchased from Sigma Chemical Co. (St. Louis, USA) unless otherwise specified. Antibodies targeting eNOS, p-eNOS (serine 1177), p-eNOS (threonine 495), Sp1 and c-Jun were purchased from Cell Signaling Technology (Danvers, USA). Antibodies targeting eNOS (serine 615) were obtained from Abcam (Cambridge, USA). C2-ceramide, protein A/G agarose, antibodies targeting PP2A-Aα/β, PP2AB56-α, and PP2A-C, CD31, Hsp90, Na^+/K^+ ATPase, Lamin B and GAPDH were purchased from Santa Cruz Biotechnology (Dallas, USA). Tanshinone IIA (Tan, 98% purity assayed by HPLC) was purchased from the Chinese Institute for Drug and Biological Product Control (Beijing, China) and dissolved in dimethyl sulfoxide (DMSO) to a stock concentration of 10 mmol/L. Final concentration of DMSO in culture media was ≤0.1%.

2.2. Animals and induction of diabetes

The experimental protocols for rats were approved by the Institutional Animal Care and Use Committee at People's Liberation Army General Hospital, and conducted in accordance with the "Guide for the Care and Use of Laboratory Animals" of the National Institute of Health in China.

8-Week (230–250 g) male Sprague–Dawley (SD) rats were provided by Jackson Laboratories (Pennsylvania, USA). Rats were fasted for 16 h before the induction of diabetes with streptozotocin (STZ). A freshly prepared solution of STZ (65 mg/kg body weight) in 0.01 mol/L sodium citrate buffer (pH 4.0) was injected intraperitoneally (i.p.) [14], and the controls were injected with an equivalent amount of sodium citrate buffer alone. The hyperglycemia was confirmed (1 week later) by measuring blood levels using a OneTouch Test Strips. Only those rats with blood glucose concentrations ≥16.7 mmol/L after STZ injection were selected as diabetic rats. Rats were randomly divided into 4 groups, with 8 in each group, as follows:

1. Control group: rats were non-diabetic rats with equal amount of sodium citrate buffer, received the same volume of DMSO.
2. Control + Tan group: rats were non-diabetic rats with equal amount of sodium citrate buffer, received Tan (0.5 mg/kg) via oral gavage once daily for 2 weeks.
3. Diabetes: rats were injected with STZ as described above, received the same volume of DMSO.
4. Diabetes + Tan: rats were injected with STZ as described above, received Tan (0.5 mg/kg) via oral gavage once daily for 2 weeks.

The concentration of Tan was selected on the basis of previous publications [15,16], and has been proved to be safe for SD rats. After 1 week following a period of Tan treatment (2 weeks), blood samples were collected to determine the level of blood glucose, blood pressure, triglyceride and total cholesterol through biochemical means or radioimmunoassay. The thoracic aortas were harvested for quantitative real-time PCR, western blot or immunofluorescent staining.

2.3. Cell culture

Human umbilical vein endothelial cells (HUVECs) were extracted and cultured as previously described [12]. In brief, HUVECs were removed from human umbilical veins by collagenase digestion and cultured in medium 199 supplemented with 20% fetal calf serum, and antibiotics (100 U/mL penicillin and 100 U/mL streptomycin). HUVECs were trypsinized and subcultured in 35-mm culture dishes, and grown to 80% confluent before treatment. Passage 3–6 HUVECs were used for experiments. In this study, cells were co-incubated with different concentrations (1, 5, 10 μmol/L) of Tan and high glucose (35 mmol/L) for 48 h unless otherwise stated.

2.4. Quantitative real-time PCR

Total RNA (1 μg) from HUVECs and aortas was isolated using the RNeasy Mini Kit (Qiagen, Hilden, Germany) according to the manufacturer's instructions and was reverse-transcribed using the ReverTra ACE qPCR RT Kit (Toyobo, Osaka, Japan). RT-PCR was performed using SYBR Green PCR master mix (Invitrogen, Grand Island, USA) with an ABI Prism 7300 Fast Real-Time PCR system (Applied Biosystems, Grand Island, USA). The eNOS mRNA expression was normalized to the mRNA levels of GAPDH. The specific primer sequences used for the amplification were as follows: eNOS (human), 5′-CCCTTC AGTGGCTGGTACAT-3′ and 5′-CACGATGGTGACTTTGGCTA-3′; eNOS (rat), 5′-TCCGATTCAACAGTGTCTCCT-3′ and 5′-ACAGAAGTGCGGGTAT GCTC-3′; GAPDH (human), 5′-GGGCACGAAGGCTCATCATT-3′ and 5′-AGAAGGCTGGGGCTCATTTG-3′; and GAPDH (rat), 5′-TGCTGGTGCTGA GTATGTCGTG-3′ and 5′-CGGAGATGATGACCCTTTTGG-3′. Reactions were carried out by 30 (eNOS) and 19 (GAPDH) cycles (95 °C for 10 s and 61 °C for 30 s) after an initial 3 min at 95 °C.

2.5. Western blot analysis

Aorta homogenates and cell extracts were subjected to western blot analysis as previously described [12]. Equal amounts of protein were separated with SDS-PAGE and then transferred onto a Polyvinylidene Fluoride (PVDF) membrane (Millipore, Billerica, USA). Blots were incubated with appropriate antibodies. Bands were visualized by ECL system (Thermo Scientific, Pittsburgh, USA) and quantified by Gel-ProAnalyzer 6.0 (Media Cybernetics Corporation, Warrendale, USA).

2.6. Immunohistochemistry

At the age of 12 weeks, rat thoracic aorta was carefully excised, and embedded and frozen using optimal cutting temperature compound (Tissue-Tek, Sakura, Japan) for immunohistochemistry. 3% hydrogen peroxide aqueous solution was applied to block endogenous peroxidase activity. The sections were blocked by 10% goat serum and incubated with rabbit-anti-eNOS (1:100 dilution) overnight at 4 °C, followed by incubation with secondary antibody for 1 h at room temperature and

3,3′ diaminobenzidine (DAB) substrate color development. Then the sections were dehydrated, cleared and examined under a Zeiss Axioplan2 fluorescence microscope (München, Germany).

2.7. Immunofluorescent staining

To detect the expression of eNOS in the aorta, frozen tissue sections were incubated with rabbit-anti-eNOS (1:100 dilution). To observe the co-localization of eNOS and PP2A-A in HUVECs, cells were fixed and labeled with rabbit-anti-eNOS and goat-anti-PP2A-A (1:200 dilution) antibodies. Samples were then washed three times with PBS for 3 min and then were incubated with appropriate secondary antibodies (anti-rabbit FITC antibody for labeling eNOS and anti-goat Cy3 antibody for labeling PP2A-A, 1:200 dilution; Jackson Laboratories) for 1 h at room temperature. Fluorescent images were acquired using the Zeiss Axioplan2 fluorescence micro

2.8. Measurement of NO generation

Intracellular levels of NO were detected using the fluorescent NO indicator, 3-amino,4-aminomethyl-2′,7′-difluorescein, diacetate (DAF-FM DA) as previously described [17]. After treatment, cells were washed with PBS and then loaded with DAF-FM DA (1 μmol/L) in serum-free medium 199 for 30 min in the dark at 37 °C. Then the fluorescence intensity of dishes was measured at 495 nm excitation and 515 nm emission by FV500 laser-scanning confocal microscopy (Olympus, Tokyo, Japan). The mean values of fluorescence intensity were from at least four independent experiments.

2.9. Enzyme Linked Immunosorbent Assay (ELISA)

Rat aortas were harvested at the age of 12 weeks. Aorta homogenates or cell extracts were prepared in 0.1 mol/L HCl (1% Triton X-100 and protease inhibitors; Merck, Darmstadt, Germany). The concentrations of cGMP or BH4 were determined using cGMP ELISA Kit (R&D Systems, Minneapolis, USA) or BH4 ELISA Kit (Xinfanbio, Shanghai, China), respectively. All measurements were performed as recommend by the manufacturer's protocol.

2.10. Measurement of nitrite and nitrate production

Nitrite (NO_2^-) and nitrate (NO_3^-) in tissue homogenates and cell extracts were measured using a total nitric oxide assay kit (Beyotime, Jiangsu, China) according to the manufacturer's recommendations. Total nitric oxide production was normalized to total proteins.

2.11. Vascular reactivity measurement

After euthanasia, the thoracic aortas were carefully isolated, and cleaned excess fat and connective tissues. The thoracic aortas were carefully cut into 2 or more rings and mounted as ring preparations (2–3 mm long) in organ bath containing modified Krebs solution (mmol/L: NaCl 137, KCl 5.4, $CaCl_2$ 2.0, $MgCl_2$ 1.1, NaH_2PO_4 0.4, $NaHCO_3$ 11.9, glucose 5.6, pH = 7.2) gassed with 95% O_2 and 5% CO_2 at 37 °C continuously. The vascular developed tension was recorded by an isometric force transducer (model 610, DMT-USA, GA, USA) and the data was converted to a computer by a PowerLab8/SP data acquisition system (AD Instruments Pty Ltd., Colorado Springs, USA). The arterial rings were stretched to a resting tension of 10 mN in bath medium, and the solution was changed every 15 min. After equilibrating for 1 h, contraction response curves for phenylephrine (PE; 10^{-9}–10^{-5} mol/L) were obtained. After repeated rinsings, the rings were precontracted with PE (10^{-5} mol/L) to reach maximal tension and endothelium-dependent relaxation was assessed by measuring the relaxation response to acetylcholine (Ach; 10^{-9}–10^{-5} mol/L). Endothelium-dependent eNOS-independent relaxation was evaluated by measuring the response to Ach after incubation with the eNOS inhibitor *Nω*-nitro-L-arginine methyl ester (L-NAME, 10^{-4} mol/L). Endothelium-independent relaxation was determined by measuring the relaxation response to sodium nitroprusside (SNP; 10^{-10}–10^{-6} mol/L).

2.12. Transient transfection and luciferase reporter gene assay

HUVECs in 6-well plates were co-transfected with pGL2–eNOS promoter-luciferase (Addgene plasmid 19297), and β-galactosidase plasmid (Promega, Madison, USA) as an internal control using Effectene Transfection Reagent (Qiagen) according to the manufacturer's instructions for 24 h, and then incubated with high glucose in the absence or presence of different concentrations of Tan for 48 h. Cell lysates were assayed for luciferase activity and β-galactosidase activity using a luciferase assay kit (Promega) as measured with a luminometer (AutoLumat Plus, Berthold Technology, Calmbacher, Germany). The luminometer reported relative light units, which were normalized by β-galactosidase activity.

2.13. Nuclear extract preparation and transcription factor translocation analysis

Nuclear protein extracts were prepared using the NucBuster Protein Extraction Kit (Novagen, Madison, USA) according to the manufacturer's instructions. Nuclear translocation of Sp1 and c-Jun was determined by western blot with Sp1 antibody and c-Jun antibody (1:500 dilution). Lamin B (1:500 dilution) was used as a nucleus internal control.

2.14. Electrophoretic mobility shift assay (EMSA)

Nuclear extract was obtained for EMSA as described above. Double-stranded oligonucleotides containing the consensus DNA binding site for AP-1 (5′-CGCTTGATGAGTCAGCCGGAA-3′) and Sp1 (5′-ATTCGATC GGGGCGGGGCGAGC-3′) were radiolabeled with [γ-^{32}P]ATP (30 μCi) by using a 5′ end labeling kit (Pierce, Illinois, USA). Nuclear proteins (10 μg) were incubated with ^{32}P-labeled oligonucleotide. Binding reactions were performed on a 4% non-denaturing polyacrylamide gel. The gel was subsequently dried and imaged by autoradiography.

2.15. Transcription factor analysis

For the analysis of transcription factors, we used the TransFactor Profiling Kit Inflammation-2 (BD Biosciences Clontech, Palo Alto, USA). 20 μg of nuclear extracts was applied into 96-well plates then coated with oligonucleotides containing the specific DNA binding sequence of several transcription factors (Sp1, c-Jun, FosB) and processed according to the manufacturer's instructions. Binding of these transcription factors was then achieved by specific primary antibody that was subsequently detected by a secondary antibody conjugated to horseradish peroxidase. The bound immunocomplex was then detected with an HRP substrate reaction, and the absorbance of the substrate was read by a spectrophotometer (Infinite F500 mMulti Reader, TECAN, Männedorf, Switzerland). Consensus sequences contained in coated oligonucleotides were as follows: GTGGGGGCGGGGC for Sp1, TGACTCA for c-Jun, and TGACTCA for FosB.

2.16. eNOS mRNA and protein stability assay

HUVECs were co-incubated with Tan (10 μmol/L) and high glucose (35 mmol/L) for 48 h, then 20 μg/mL 5,6-dichloro-1-β-D-ribofuranosylbenzimidazole (DRB) or 10 μg/mL cycloheximide (CHX) was added for different times as indicated (0, 8, 16, 24 h). eNOS mRNA and protein levels were determined by RT-PCR and western blot as described above, respectively.

2.17. Immunoprecipitation

The thoracic aortas were homogenized in RIPA buffer and centrifuged at 1000 ×*g* for 10 min. Triton X-100 was added to the supernatant to a final concentration of 1% and was incubated for 30 min at 4 °C. The extracts were then centrifuged at 12,000 ×*g* for 15 min. The samples were precleared nonspecific binding with protein A/G agarose beads. The precleared supernatants were then co-incubated with appropriate antibodies and protein A/G agarose beads at 4 °C overnight. Beads were washed extensively with RIPA buffer/1% Triton X-100 and boiled in SDS sample buffer for western blot analysis using appropriate antibodies.

2.18. Superoxide measurements

Frozen thoracic aorta slides were stained by dihydroethidium (DHE, 5 μmol/L) in a humidified chamber in the dark at 37 °C for 30 min. Then the slides were washed three times and quickly imaged with a fluorescent microscope (Olympus, Tokyo, Japan) at 325 nm excitation and 610 nm emission keeping the same exposure for every section.

2.19. eNOS activity assay

eNOS activity was measured by the [^{3}H]-L-arginine to [^{3}H]-citrulline conversion assay [18]. To determine the activity of phospho-eNOS, the conversion was measured in the presence of 1 mmol/L $CaCl_2$ with a NOS assay kit (Merck) according to the manufacturer's instructions.

2.20. Phosphatase activity assay

Cells were lysed with phosphatase lysis buffer (50 mmol/L Tris–HCl, 1 mmol/L EDTA, 2 mmol/L dithiothreitol and 1% cocktail, pH = 7.4). eNOS immunoprecipitates were prepared as describe above. Activities of PP2A in cell lysis or eNOS immunoprecipitates were determined by using a malachite green phosphatase assay protocol as previously described [19]. A phosphopeptide (KRpTIRR; pT is phosphorylated threonine) was used as a substrate (Upstate Biotechnology, NY, USA) and the absorbance of the substrate was measured with an Infinite F500 mMulti Reader spectrophotometer at 650 nm.

2.21. Cell fractionation

Cell fractionation was performed as previously reported with some modifications [19]. Cells were lysed with lysis buffer (150 mmol/L NaCl, 100 mmol/L Tris, pH 7.4 and 1% cocktail) and then centrifuged at 12,000 ×*g* for 15 min. Cytoplasmic and membrane fractions were separated from the supernatant by ultracentrifugation at 43,000 ×*g* for 60 min and resuspended in lysis buffer prior to analyses by western blot.

2.22. Statistical analysis

All data were expressed as mean ± SEM. The one-way analysis of variance (ANOVA) or an unpaired two-tailed Student t test was used to analyze the differences between groups. A level of $P < 0.05$ was considered significant in all statistical tests.

3. Results

3.1. General parameters

To determine the protective role of Tan in the pathological process of diabetes, we conducted with a pharmacological approach of Tan (0.5 mg kg^{-1} d^{-1}) as schematically illustrated in Fig. S1. Injection of STZ showed a significant reduction in body weight and a marked increase in blood glucose, blood pressure and total cholesterol. Administration of Tan for 2 weeks resulted in more than 50% reduction in blood pressure compared with diabetes group. However, Tan treatment seemed not be able to modulate the other parameters (Table 1).

3.2. Tan attenuated the decrease of eNOS expression induced by diabetes/high glucose

Under basal level, the protein and mRNA levels of eNOS were both enhanced in the aortas isolated from Tan-treated rats compared to vehicle-treated rats. Consistent with previous studies [20–22], we found that eNOS expression was significantly decreased in the aortas isolated from diabetic rats in a time-dependent manner, which started from 2 weeks (Fig. S2A–B). However, these reductions were all attenuated after Tan administration (Fig. 1A–B). Fig. 1C–D showed sections from rat aortas, taken from normal (control) or diabetic rats before and after Tan administration. Immunohistochemistry studies on these sections using an antibody against eNOS revealed that Tan treatment increased the existing eNOS under basal level. After injected with STZ intraperitoneally for 4 weeks, the existing eNOS was significantly decreased compared with control. However, this reduction was ameliorated following Tan treatment (Fig. 1C). As expected, inspection with fluorescence microscopy showed similar patterns of eNOS staining (Fig. 1D). Additionally, treatment with Tan obviously attenuated high glucose-induced decrease of eNOS expression at both protein and mRNA levels in HUVECs, similar to what was observed in diabetic rats (Fig. 1E–F).

3.3. Tan ameliorated diabetes-induced decrease of NO generation and impairment of endothelium-dependent vasorelaxation

To investigate whether the upregulation of eNOS expression following Tan treatment could result in an increase of NO generation, cGMP and nitrite concentrations were measured. Under basal level, cGMP and nitrite concentrations were both increased significantly in Tan-treated rats compared to vehicle-treated rats. Diabetic rats presented a sharp decrease in NO generation, which was almost completely abolished in Tan-treated diabetic rats (Fig. 2A–B).

To determine if our in vivo findings were operative in vitro, the intracellular NO content in HUVECs was assayed by measuring the intensity of DAF-FM DA fluorescence. Compared with control group, fluorescence intensity after high glucose challenge was significantly decreased, but osmotic control (mannitol) produced no effect on fluorescence intensity (Fig. S3A). Incubation of HUVECs with Tan (1, 5, 10 μmol/L) in the presence of high glucose attenuated the decrease of NO content in a concentration-dependent manner (Fig. S3B). Expectedly, Tan obviously ameliorated high glucose-induced decrease of cGMP and nitrite concentrations in HUVECs in a concentration-dependent manner, similar to what was observed in vivo (Fig. 2C–D). These pharmacological results suggest that Tan inhibits diabetes/high glucose-induced decrease of NO generation.

Table 1
Effect of administration of Tanshinone IIA (0.5 mg/kg) on physiological parameters.

Parameter	Control	Control + Tan	Diabetes	Diabetes + Tan
Body weight (g)	252.6 ± 12.5	244.9 ± 14.1	196.8 ± 16.4*	207.5 ± 17.1*
Blood glucose (mmol/L)	11.9 ± 1.3	12.1 ± 1.4	23.5 ± 1.5**	23.0 ± 1.2**
Blood pressure (mm Hg)	103.5 ± 3.9	105.1 ± 4.1	156.2 ± 4.7**	129.3 ± 3.9##
TG (mmol/L)	1.38 ± 0.38	1.22 ± 0.46	2.37 ± 0.51*	2.54 ± 0.52*
TC (mmol/L)	2.98 ± 0.66	3.32 ± 0.81	2.78 ± 0.54	3.07 ± 0.81

TG, triglyceride; TC, total cholesterol.
* $P < 0.05$.
** $P < 0.01$ vs. control.
$P < 0.01$ vs. diabetes.

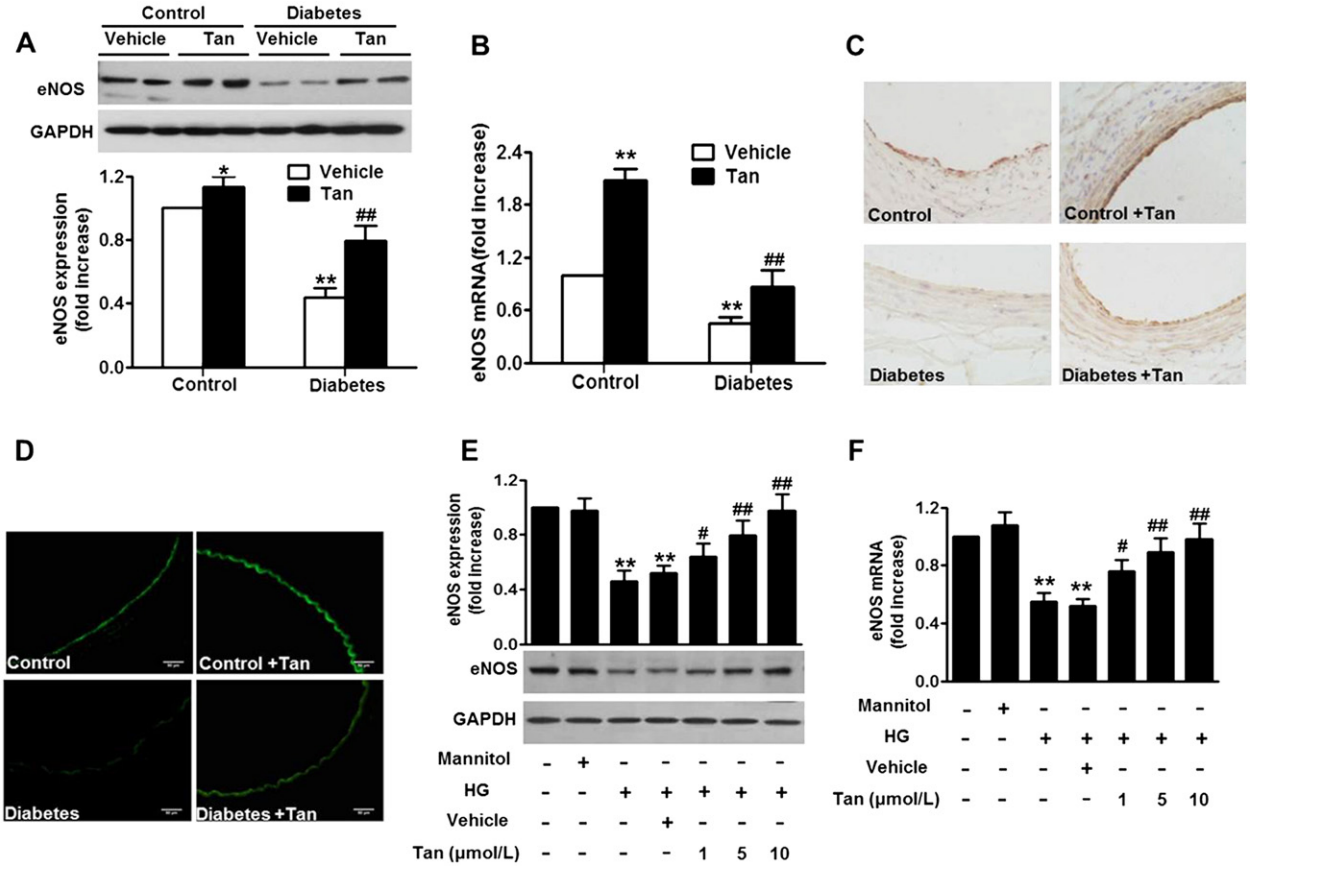

Fig. 1. Tan attenuates diabetes/high glucose-induced decrease of eNOS expression. A and B, Western blot (A) and quantitative PCR (B) analyses of eNOS protein and mRNA expression, respectively. n = 6/group, $^{*}P < 0.05$, $^{**}P < 0.01$ vs. control + vehicle; $^{\#\#}P < 0.01$ vs. diabetes + vehicle. C and D, The expression of eNOS in the aorta was analyzed by immunohistochemistry (C) and immunofluorescent staining (D). E and F, HUVECs were co-incubated with high glucose and different concentrations (1, 5, 10 μmol/L) of Tan for 48 h. eNOS expression was examined by western blot (E) and quantitative PCR (F), respectively. n = 4, $^{**}P < 0.01$ vs. control; $^{\#}P < 0.05$, $^{\#\#}P < 0.01$ vs. HG.

To examine whether Tan-increased NO generation would offer a protective effect on endothelial relaxing dysfunction in diabetes, the response of the thoracic aortas to the endothelium-dependent vasodilator acetylcholine (Ach; 10^{-9}–10^{-5} mol/L) was tested. Under basal level, although the concentration–response curves to Ach were similar in these two groups, the thoracic aortas from Tan-treated rats presented a modest reduction of ED50 compared to vehicle-treated rats (0.08 ± 0.01 nmol/L vs. 0.18 ± 0.02 nmol/L, $P < 0.01$, Fig. 2E). Compared to vehicle-treated rats, Ach-induced endothelium-dependent relaxation in the thoracic aortas from diabetic rats was impaired in a time-dependent manner (Fig. S4A). However, this impairment was significantly improved in Tan-treated diabetic rats (Fig. 2E). *Nω*-nitro-L-arginine methyl ester (L-NAME; 10^{-4} mol/L) almost completely eliminated Ach-induced vasorelaxation, and endothelium-independent vasorelaxation in response to sodium nitroprusside (SNP; 10^{-10}–10^{-6} mol/L) exhibited no difference for any of these groups (Fig. S4B–C). However, the phenylephrine (PE; 10^{-9}–10^{-5} mol/L)-induced contractile responses seemed similar in all groups and no difference was observed (Fig. 2F). Together, these data imply that administration of Tan improves endothelium-dependent dilatation under basal level and diabetes.

3.4. Effects of Tan on eNOS transcriptional activity and mRNA half-life after high glucose challenge

To investigate whether the upregulation of eNOS expression following Tan treatment occurs simply at eNOS transcriptional level, we measured eNOS transcriptional activity. Our results showed that high glucose significantly inhibited eNOS transcriptional activity in HUVECs. However, Tan failed to inhibit this effect (Fig. 3A). To investigate whether the decrease in eNOS transcriptional activity was associated with a reduced binding activity of the transcription factors Sp1 and AP-1, electrophoretic mobility shift assays were performed. As shown in Fig. 3B, when nuclear proteins extracted from high glucose-treated cells were incubated with oligonucleotides corresponding to the Sp-1 binding sequences, decreased binding activity occurred. Simultaneous exposure of HUVECs to Tan produced no effect on Sp1 binding activity. Similar results were obtained in AP-1 binding assay. We next sought to determine the possible transcription factors involved. ELISA analysis showed that the nuclear translocation of Sp1 and c-Jun was significantly inhibited following high glucose stimulation in HUVECs, whereas FosB was not affected (Fig. 3C), indicating a role of decreased AP-1 binding via c-Jun but not FosB in the decrease of eNOS promoter activity after high glucose challenge. This was further supported by the nuclear expression of Sp1 and c-Jun in HUVECs (Fig. S5A–B).

Because Tan did not ameliorate high glucose-induced decrease of eNOS transcriptional activity, a post-transcriptional regulation seemed to be taking place. eNOS mRNA stability was investigated in HUVECs using a transcriptional inhibitor, 5,6-dichloro-1-β-D-ribofuranosylbenzimidazole (DRB, 20 μg/mL). Our results showed that no significant difference was found in eNOS mRNA decay ratio between control group and high glucose group. However, Tan significantly increased eNOS mRNA half-life from <15 h to ≈24 h (Fig. 3D), indicating that eNOS mRNA stabilization underlies the protective effects of Tan on eNOS expression.

3.5. Analysis of the post-translational mechanism involved in eNOS upregulation by Tan

We next examined eNOS protein half-life by using a protein synthesis inhibitor, cycloheximide (CHX, 10 μg/mL). Consistent with previous

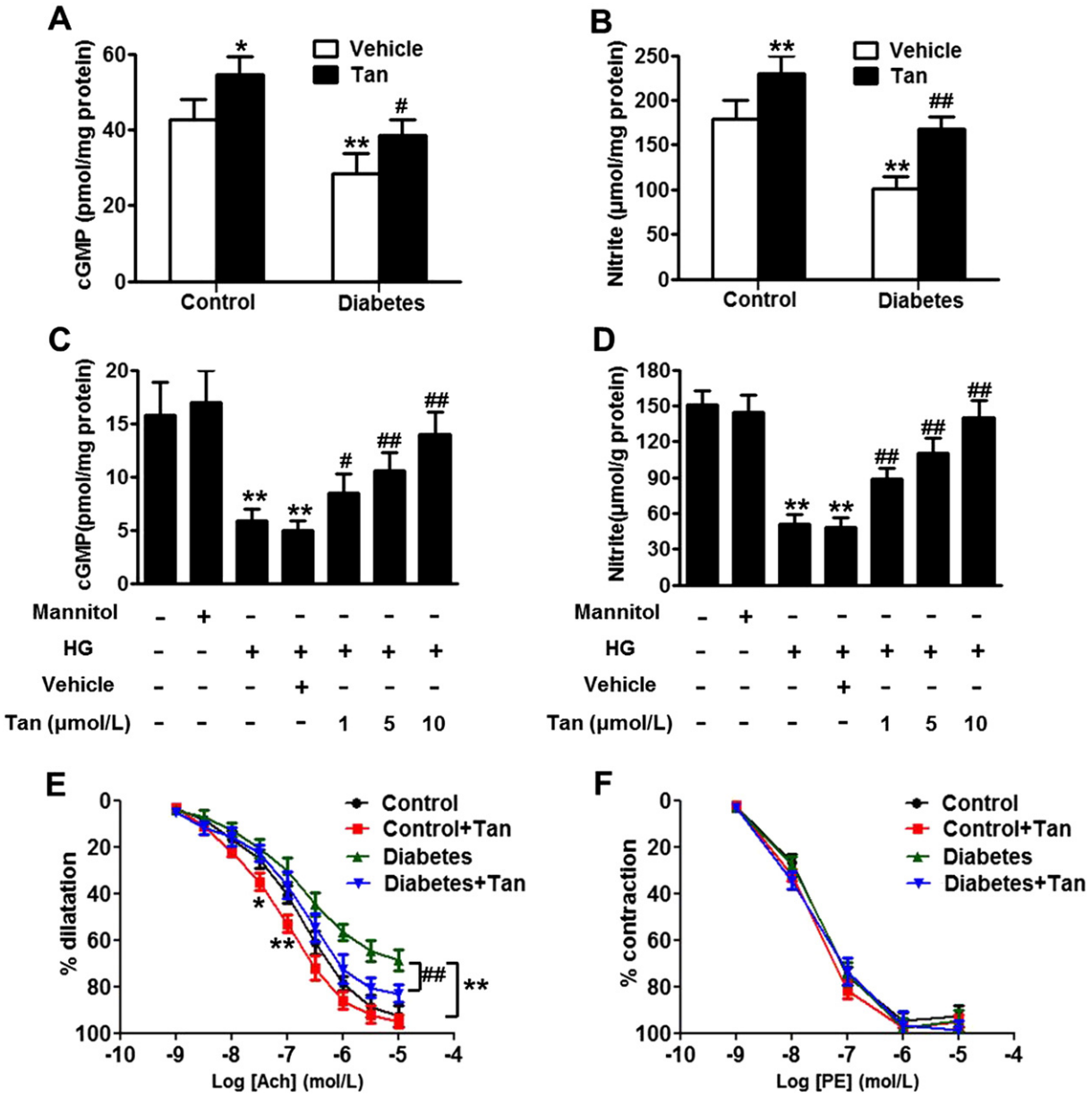

Fig. 2. Tan ameliorates the impairment of NO generation and endothelium-dependent vasorelaxation. A and B, Levels of NO generation in tissue homogenates of control and diabetic rats before and after Tan administration were determined by measuring cGMP (A) and nitrite plus nitrate accumulation (B). n = 6/group, $^{*}P < 0.05$, $^{**}P < 0.01$ vs. control + vehicle; $^{\#}P < 0.05$, $^{\#\#}P < 0.01$ vs. diabetes + vehicle. C and D, HUVECs were stimulated with high glucose in the presence or absence of Tan for 48 h. cGMP (C) and nitrite plus nitrate accumulation (D) were determined. n = 4, $^{**}P < 0.01$ vs. control; $^{\#}P < 0.05$, $^{\#\#}P < 0.01$ vs. HG. E, Vascular reactivity in vehicle-treated, Tan-treated, vehicle-treated diabetic and Tan-treated diabetic rats was measured to visualize vasodilation of the thoracic aorta in response to acetylcholine (Ach; 10^{-9}–10^{-5} mol/L) after preconstruction with phenylephrine (PE; 10^{-5} mol/L). F, Concentration–response curves to PE (10^{-9}–10^{-5} mol/L). n = 8/group, $^{*}P < 0.05$, $^{**}P < 0.01$ vs. control + vehicle; $^{\#\#}P < 0.01$ vs. diabetes + vehicle.

results [23], CHX treatment showed a time-dependent decrease of eNOS protein level in HUVECs. Compared to control group, high glucose significantly increased the rate of eNOS degradation, shortening eNOS protein half-life by more than 4 h. In contrast, Tan (10 μmol/L) antagonized against the degradation of eNOS induced by high glucose (Fig. 4A), suggesting that the Tan-induced upregulation of eNOS expression requires de novo protein synthesis. This was further supported by the result of eNOS ubiquitination (Fig. S6).

To further explore the mechanisms by which Tan upregulates eNOS expression at post-translational level, we investigated the effect of Tan on eNOS uncoupling. Consistent with a previous report [8], high glucose stimulation exhibited a decrease of eNOS dimer/monomer ratio in HUVECs, which has been associated with eNOS uncoupling. However, Tan significantly increased the ratio of eNOS dimer to monomer (Fig. 4B). Because eNOS uncoupling results in an increase of eNOS-derived superoxide anion (O_2^-) and recently was reported as a consequence of reduced BH4 concentration or Hsp90/eNOS complex formation [13,23], we found that Tan inhibited diabetes-induced increase of O_2^- and decrease of BH4 concentration and Hsp90/eNOS interaction in the aortas (Figs. 4C–D, S7).

Phosphorylation of eNOS has been known to be the central post-translational mechanism of eNOS regulation. Although the level of total eNOS was decreased by high glucose, eNOS serine 1177 phosphorylation was reduced more obviously in HUVECs; this was almost abolished after Tan treatment (Fig. 4E). Moreover, according to the changes in total eNOS expression, phosphorylation status of threonine 495 or serine 615 was not altered following high glucose stimulation (Fig. 4F), indicating that high glucose-induced serine 1177 dephosphorylation was a specific event. Similar result was obtained from the analysis of phospho-eNOS activity by measuring the arginine to citrulline

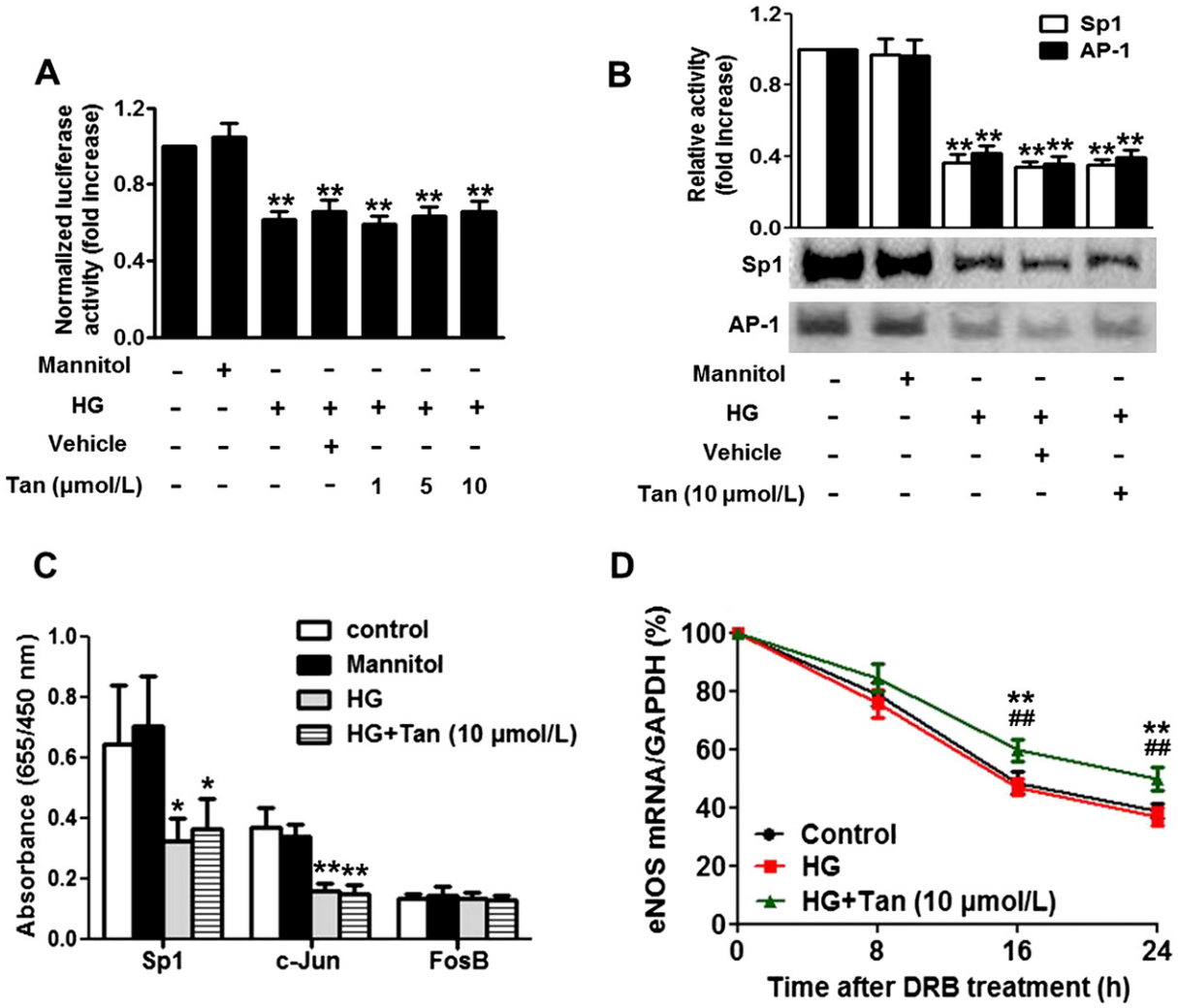

Fig. 3. Effects of Tan on eNOS transcriptional activity and mRNA half-life in the presence of high glucose. HUVECs were stimulated with high glucose in the presence or absence of Tan for 48 h. A, Luciferase assay for HUVECs co-transfected with pGL2–eNOS promoter plasmid and β-galactosidase plasmid. Luciferase activity was normalized by β-galactosidase activity. B, The binding activity of Sp1 and AP-1 was determined by electrophoretic mobility shift assay. Densitometric analysis of the autoradiographs was performed. C, Nuclear translocation analysis of transcription factors Sp1, c-Jun and FosB. D, After treatment, DRB (20 μg/mL) was added for the indicated times, and eNOS mRNA levels were analyzed by quantitative PCR. Graph showing the effect of DRB on eNOS steady-state mRNA level. All data are presented as mean ± SEM. n = 4–6, $^{*}P < 0.05$, $^{**}P < 0.01$ vs. control; $^{\#\#}P < 0.01$ vs. HG.

conversion assay (Fig. S8A). Collectively, these data indicate that Tan regulates eNOS expression and activity by multiple mechanisms at post-translational level.

3.6. Tan prevented high glucose-induced dephosphorylation of eNOS through impairing PP2A-A translocation and PP2A-A/eNOS interaction

Because PP2A has been suggested to dephosphorylate eNOS at serine 1177, we investigated whether PP2A is involved in high glucose-induced eNOS serine 1177 dephosphorylation. As shown in Fig. 5A, incubation of HUVECs with okadaic acid (50 nmol/L), an inhibitor of PP2A, reversed high glucose-induced eNOS dephosphorylation. However, the effect of Tan on eNOS dephosphorylation was almost abolished by adding C2-ceramide (10 μmol/L), an agonist of PP2A. As a result, C2-ceramide displayed similar effect on phospho-eNOS activity (Fig. S8B). These date indicate that PP2A is involved in Tan-mediated eNOS phosphorylation.

We further investigated the effect of Tan on PP2A expression in HUVECs. Interestingly, neither high glucose nor Tan produced significant effect on PP2A (PP2A-A, B, C) expression (Fig. S9A). To exclude the possibility that Tan changes PP2A activity, phospho-PP2A activity was measured. As shown in Fig. S9B, PP2A activity was not affected by high glucose and Tan in HUVECs. Therefore, decreased PP2A expression or attenuated catalytic activity is not required for Tan-reversed eNOS dephosphorylation.

Given that eNOS is a membrane-associated enzyme, we speculated that Tan may be involved in regulating PP2A subcellular localization. Western blot results showed PP2A-A mainly resided in the cytosol of HUVECs under basal level. An obvious increase of PP2A-A content was observed in the membrane fractions following high glucose stimulation, suggesting that the enrichment of PP2A-A membrane may be one of the contributors for the high glucose-induced eNOS dephosphorylation. However, Tan significantly inhibited the translocation of PP2A-A. Although the endogenous expression of eNOS is faint in the cytosol, Tan also significantly inhibited high glucose-induced decrease of eNOS expression, which was in line with the changes of total protein expression. We found that eNOS expression in the membrane was not affected. This is probably because eNOS is already highly abundant in the membrane. Notably, no significant differences were observed on the distribution of PP2A-B and PP2A-C in cytosolic and membrane fractions, indicating that Tan-impaired PP2A-A translocation is a highly specific event (Fig. 5B–C).

Confocal microscopy of HUVECs revealed PP2A-A predominantly expressed at the plasma membrane in HUVECs. A similar pattern for

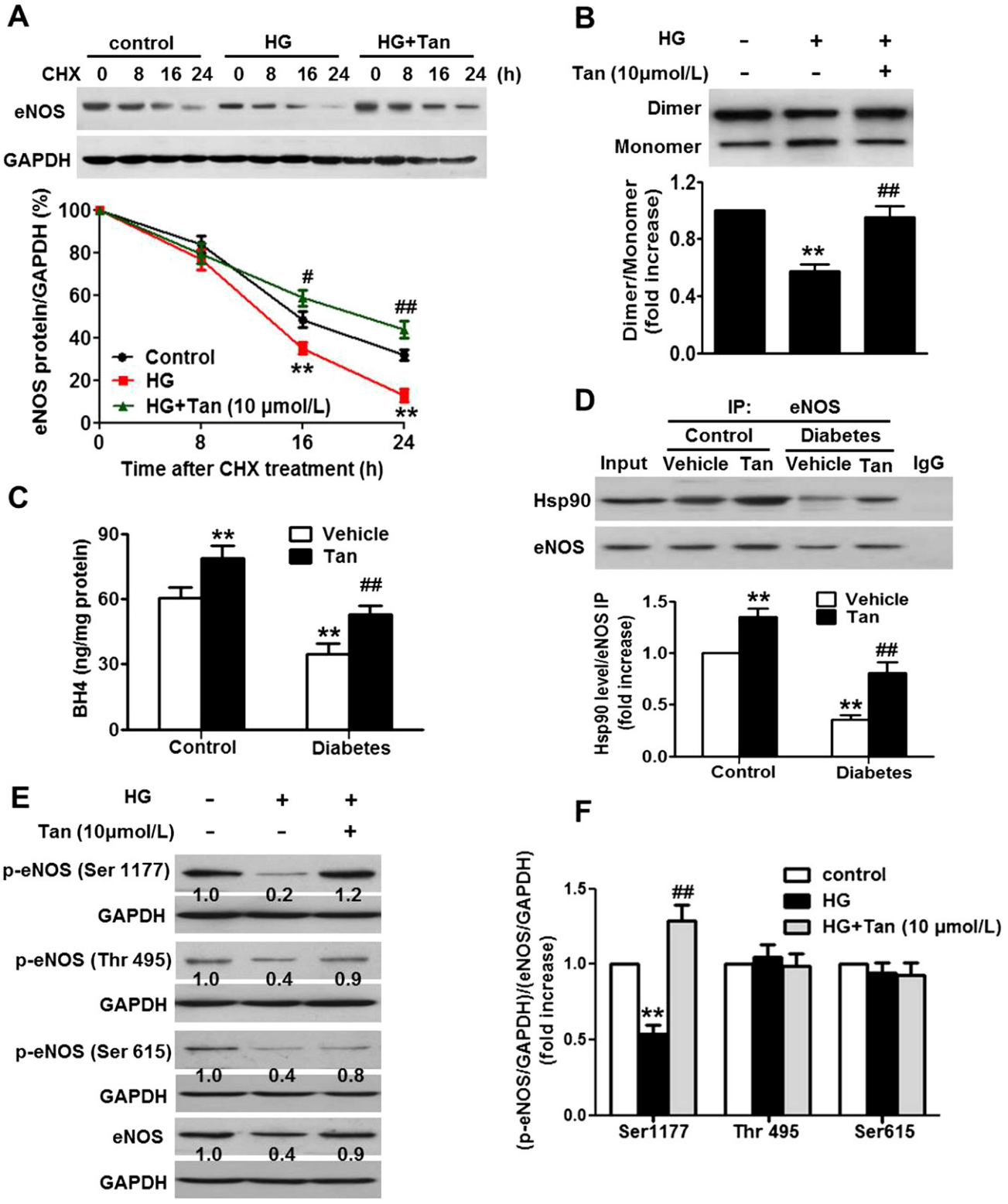

Fig. 4. The post-translational mechanisms involved in eNOS upregulation by Tan. A, HUVECs were stimulated with high glucose in the presence or absence of Tan (10 μmol/L) for 48 h. After treatment, CHX (10 μg/mL) was added for the indicated times. Representative blot corresponding to eNOS protein levels was shown. B, eNOS dimer–monomer levels were determined by low temperature gel electrophoresis. n = 4, $^{**}P < 0.01$ vs. control; $^{\#}P < 0.05$, $^{\#\#}P < 0.01$ vs. HG. C, BH4 concentrations in the aorta homogenates were measured. D, Immunoblotting for Hsp90 or eNOS after immunoprecipitation (IP) with eNOS antibody in the thoracic aorta homogenates of control and diabetic rats before and after Tan administration (n = 5–7/group). $^{*}P < 0.05$, $^{**}P < 0.01$ vs. control + vehicle; $^{\#\#}P < 0.01$ vs. diabetes + vehicle. E and F, eNOS serine 1177, threonine 495, and serine 615 phosphorylation and eNOS activity were examined (E), and densitometric analysis was performed (F). n = 6, $^{**}P < 0.01$ vs. control; $^{\#\#}P < 0.01$ vs. HG.

eNOS was observed, and image superimposition showed marked co-localization of the PP2A-A and eNOS (Fig. 5D). In addition, immunoprecipitation with PP2A-A resulted in a co-precipitation of eNOS (Fig. 5E). These data further confirmed that eNOS interacted with PP2A-A in HUVECs. To ascertain whether this PP2A-A/eNOS interaction is regulated by Tan, we immunoprecipitated with eNOS and characterized the

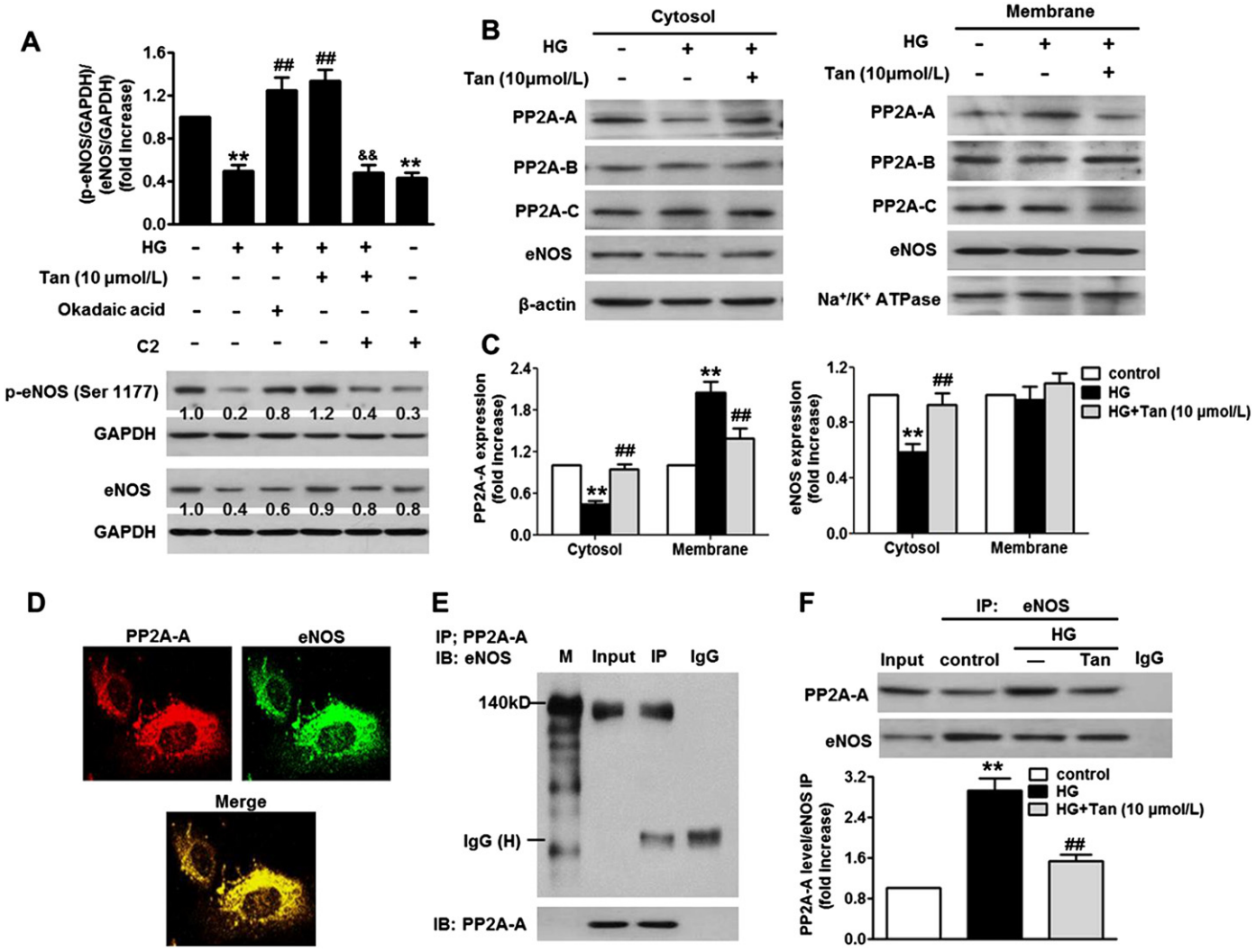

Fig. 5. Tan inhibits high glucose-induced PP2A-A translocation and PP2A-A/eNOS interaction. HUVECs were stimulated with high glucose in the presence or absence of Tan (10 μmol/L) for 48 h. A, Okadaic acid (50 nmol/L) or C2-ceramide (C2, 10 μmol/L) was added 1 h before the treatment mentioned above. eNOS serine 1177 phosphorylation was detected by western blot. B, The content of PP2A subunits (PP2A-A, B, C) and eNOS in the cytoplasm and membrane in HUVECs were detected by western blot. Na^+/K^+ ATPase was used an internal control of membrane. C, Densitometric quantification of PP2A-A and eNOS levels in (B) normalized to corresponding internal control. D, Representative images of eNOS and PP2A-A distribution in normal HUVECs. E, Immunoprecipitation (IP) of PP2A-A resulted in a co-precipitation of eNOS in HUVECs. F, Immunoblotting (IB) for PP2A-A or eNOS after immunoprecipitation (IP) with PP2A-A antibody. All data are presented as mean ± SEM. n = 4–6, $^{**}P < 0.01$ vs. control; $^{\#\#}P < 0.01$ vs. HG; $^{\&\&}P < 0.01$ vs. HG + Tan.

PP2A-A protein abundance in the immunoprecipitated proteins. As expected, PP2A-A was found in eNOS immunoprecipitated proteins in HUVECs and high glucose significantly enhanced PP2A-A/eNOS complex formation. After Tan treatment, the increased PP2A-A/eNOS interaction was attenuated (Fig. 5F). Consistent with previous data, Tan decreased phospho-PP2A activity in eNOS immunoprecipitated proteins, as compared with high glucose-treated cells (Fig. S9C). Together, these data suggest that Tan inhibits high glucose-induced PP2A-A/eNOS complex formation, leading to prevent eNOS dephosphorylation.

4. Discussion

Endothelial dysfunction is an important maker of many known cardiovascular diseases, such as atherosclerosis, hypertension and diabetes [24,25]. Impairment of endothelium-dependent vasorelaxation accompanied by a reduction in nitric oxide (NO) bioavailability has been implicated as a common feature of endothelial dysfunction in the pathogenesis of diabetes [26]. In the present study, we found Tan treatment ameliorated the decrease of eNOS protein and mRNA levels in diabetic rats and high glucose condition. Of note, a study showed neither high glucose nor Tan changed total eNOS expression in endothelial cell line EA.hy926 [13]. The varied results may be due to different cell-type-specific responses. Moreover, not only by cGMP ELISA testing, but also by the detection of nitrite plus nitrate production that rapidly metabolized from NO, Tan attenuated the decrease of NO generation. It has been demonstrated that diabetes patients invariably show an impairment of endothelium-dependent vasorelaxation, which is frequently defined as a surrogate endpoint for endothelial dysfunction [24]. Here, we found that the administration of Tan improved endothelium-dependent relaxation in rat thoracic aortas under normal condition and diabetes. These data further support the critical role of Tan in maintaining endothelial homeostasis.

Regulation of eNOS expression can occur at transcriptional, post-transcriptional and post-translational levels [2]. We firstly investigated the effect of Tan on eNOS promoter activity. Although Tan ameliorated high glucose-induced decrease of eNOS mRNA expression, it did not exhibit any effects on eNOS promoter activity. Sp1 and AP-1 are known to regulate eNOS transcriptional activation via binding to its promoters, leading to increase eNOS mRNA expression [27]. Typically, AP-1 complex is a dimer of c-Jun and FosB, since it was found to supershift with anti-c-Jun and anti-FosB antibodies [27]. In addition, recent study has suggested that modulation of c-Jun expression in endothelial cells

regulates eNOS expression [28]. In the present study, we noticed a decreased binding activity of the transcription factors Sp1 and AP-1 after high glucose treatment. More interestingly, high glucose decreased the nuclear translocation of c-Jun and Sp1, but FosB was not affected. Expectedly, neither the binding activity nor translocation was affected by Tan treatment. These data suggest that the impairment of Sp1 and c-Jun (not FosB) binding activity and translocation underlies, at least in part, the inhibitory effect of high glucose on eNOS mRNA expression. At post-transcriptional level, multiple pro-inflammatory cytokines have been suggested to decrease eNOS expression by destabilizing mRNA, including LPS, TNF-α, and IL-1β [29]. Notably, unlike such inflammatory activators, eNOS mRNA stability was not affected by high glucose, but was obviously increased after Tan treatment.

In addition to transcriptional and post-transcriptional mechanisms, it is well known that eNOS activity is mainly regulated by several ways of post-translational mechanism, including protein degradation, reversible coupling, protein–protein interaction and phosphorylation [2,3]. In this study, cycloheximide treatment showed that Tan inhibited high glucose-induced eNOS degradation, and immunoprecipitation study directly demonstrated that Tan attenuated high glucose-induced eNOS ubiquitination. Consistent with these previous reported results [12,13], we found that Tan increased BH4 concentration and Hsp90/eNOS interaction to prevent eNOS uncoupling, leading to decrease eNOS-derived O_2^- in diabetic rats. Furthermore, Tan treatment specifically inhibited high glucose-induced dephosphorylation of eNOS serine 1177 in HUVECs, because the phosphorylation level of threonine 497 or serine 635 was unchanged.

PP2A is a ubiquitous serine/threonine phosphatase, which is often thought to dephosphorylate proteins with poor substrate specificity [30]. Notably, evidence has been suggested that PP2A-induced eNOS dephosphorylation specifically occurred at serine 1177 but not threonine 497, because the later was selectively dephosphorylated by protein phosphatase 1 (PP1) [31]. We found that treatment with PP2A agonist C2-ceramide completely abolished the inhibitory effect of Tan on eNOS dephosphorylation, indicating that PP2A may be a molecular target for Tan in regulating eNOS phosphorylation. Of interest, Tan-inhibited eNOS dephosphorylation was due to the impairment of PPA2-A translocation rather than the inhibition of all there subunits of PP2A expression and activity. Subsequently, Tan treatment suppressed high glucose-induced PP2A-A/eNOS complex formation, leading to prevent serine 1177 dephosphorylation.

Our data provided novel mechanisms for Tan in regulating vasorelaxation and this medicine may be a potential therapeutic agent for cardiovascular complications of diabetes.

5. Conclusion

In summary, we concluded that Tan treatment ameliorates diabetes-induced impairment of endothelium-dependent vasorelaxation via enhancing eNOS expression and activity. This action was initiated at eNOS post-transcriptional level through multiple mechanisms including regulation of eNOS mRNA and protein stability, coupling and serine 1177 phosphorylation. Our new findings may help to better understand the cardiovascular protective action of Tan.

Acknowledgements

None.

Appendix A. Supplementary data

Supplementary data to this article can be found online at http://dx.doi.org/10.1016/j.bbagen.2015.01.007.

References

[1] R.E. Gilbert, The endothelium in diabetic nephropathy, Curr. Atheroscler. Rep. 16 (2014) 410.
[2] V. Stangl, M. Lorenz, S. Meiners, A. Ludwig, C. Bartsch, M. Moobed, A. Vietzke, H.T. Kinkel, G. Baumann, K. Stangl, Long-term up-regulation of eNOS and improvement of endothelial function by inhibition of the ubiquitin–proteasome pathway, FASEB J. 18 (2004) 272–279.
[3] C.D. Searles, Transcriptional and posttranscriptional regulation of endothelial nitric oxide synthase expression, Am. J. Physiol. Cell Physiol. 291 (2006) C803–C816.
[4] P.A. Marsden, H.H. Heng, S.W. Scherer, R.J. Stewart, A.V. Hall, X.M. Shi, L.C. Tsui, K.T. Schappert, Structure and chromosomal localization of the human constitutive endothelial nitric oxide synthase gene, J. Biol. Chem. 268 (1993) 17478–17488.
[5] J. Shi, X. Wang, J. Qiu, Q. Si, R. Sun, H. Guo, Q. Wu, Roles of NF-kappaB and SP-1 in oxidative stress-mediated induction of platelet-derived growth factor-B by TNFalpha in human endothelial cells, J. Cardiovasc. Pharmacol. 44 (2004) 26–34.
[6] A. Sen, S. Ren, C. Lerchenmüller, J. Sun, N. Weiss, P. Most, K. Peppel, MicroRNA-138 regulates hypoxia-induced endothelial cell dysfunction by targeting S100A1, PLoS ONE 8 (2013) e78684.
[7] D.M. Greif, R. Kou, T. Michel, Site-specific dephosphorylation of endothelial nitric oxide synthase by protein phosphatase 2A: evidence for crosstalk between phosphorylation sites, Biochemistry 41 (2002) 15845–15853.
[8] W. Wang, L.L. Zheng, F. Wang, Z.L. Hu, W.N. Wu, J. Gu, J.G. Chen, Tanshinone IIA attenuates neuronal damage and the impairment of long-term potentiation induced by hydrogen peroxide, J. Ethnopharmacol. 134 (2010) 147–155.
[9] J.Y. Han, J.Y. Fan, Y. Horie, S. Miura, D.H. Cui, H. Ishii, T. Hibi, H. Tsuneki, I. Kimura, Ameliorating effects of compounds derived from *Salvia miltiorrhiza* root extract on microcirculatory disturbance and target organ injury by ischemia and reperfusion, Pharmacol. Ther. 117 (2008) 280–295.
[10] A. Yagi, K. Fujimoto, K. Tanonaka, K. Hirai, S. Takeo, Possible active components of tan-shen (*Salvia miltiorrhiza*) for protection of the myocardium against ischemia-induced derangements, Planta Med. 55 (1989) 51–54.
[11] D.D. Kim, F.A. Sánchez, R.G. Durán, T. Kanetaka, W.N. Durán, Endothelial nitric oxide synthase is a molecular vascular target for the Chinese herb Danshen in hypertension, Am. J. Physiol. Heart Circ. Physiol. 292 (2007) H2131–H2137.
[12] H.J. Hong, F.L. Hsu, S.C. Tsai, C.H. Lin, J.C. Liu, J.J. Chen, T.H. Cheng, P. Chan, Tanshinone IIA attenuates cyclic strain-induced endothelin-1 expression in human umbilical vein endothelial cells, Clin. Exp. Pharmacol. Physiol. 39 (2012) 63–68.
[13] Z.W. Zhou, X.L. Xie, S.F. Zhou, C.G. Li, Mechanism of reversal of high glucose-induced endothelial nitric oxide synthase uncoupling by tanshinone IIA in human endothelial cell line EA.hy926, Eur. J. Pharmacol. 697 (2012) 97–105.
[14] S. Mäkimattila, A. Virkamäki, P.H. Groop, J. Cockcroft, T. Utriainen, J. Fagerudd, H. Yki-Järvinen, Chronic hyperglycemia impairs endothelial function and insulin sensitivity via different mechanisms in insulin-dependent diabetes mellitus, Circulation 94 (1996) 1276–1282.
[15] L. Cui, T. Wu, Y.Y. Liu, Y.F. Deng, C.M. Ai, H.Q. Chen, Tanshinone prevents cancellous bone loss induced by ovariectomy in rats, Acta Pharmacol. Sin. 25 (2004) 678–684.
[16] A.M. Wang, S.H. Sha, W. Lesniak, J. Schacht, Tanshinone (*Salviae miltiorrhizae* extract) preparations attenuate aminoglycoside-induced free radical formation in vitro and ototoxicity in vivo, Antimicrob. Agents Chemother. 47 (2003) 1836–1841.
[17] L. Yao, P. Lu, Y. Li, L. Yang, H. Feng, Y. Huang, D. Zhang, J. Chen, D. Zhu, Osthole relaxes pulmonary arteries through endothelial phosphatidylinositol 3-kinase/Akt–eNOS–NO signaling pathway in rats, Eur. J. Pharmacol. 699 (2013) 23–32.
[18] J.A. Leopold, A. Dam, B.A. Maron, A.W. Scribner, R. Liao, D.E. Handy, R.C. Stanton, B. Pitt, J. Loscalzo, Aldosterone impairs vascular reactivity by decreasing glucose-6-phosphate dehydrogenase activity, Nat. Med. 13 (2007) (13 189–197).
[19] Q. Wei, Y. Xia, Proteasome inhibition down-regulates endothelial nitric-oxide synthase phosphorylation and function, J. Biol. Chem. 281 (2006) 21652–21659.
[20] F.A. Cicek, H.B. Kandilci, B. Turan, Role of ROCK upregulation in endothelial and smooth muscle vascular functions in diabetic rat aorta, Cardiovasc. Diabetol. 12 (2013) 51.
[21] A.E. Valsecchi, S. Franchi, A.E. Panerai, A. Rossi, P. Sacerdote, M. Colleoni, The soy isoflavone genistein reverses oxidative and inflammatory state, neuropathic pain, neurotrophic and vasculature deficits in diabetes mouse model, Eur. J. Pharmacol. 650 (2011) 694–702.
[22] Y. Han, X. Li, S. Zhou, G. Meng, Y. Xiao, W. Zhang, Z. Wang, L. Xie, Z. Liu, H. Lu, Y. Ji, 17β-Estradiol antagonizes the down-regulation of ERα/NOS-3 signaling in vascular endothelial dysfunction of female diabetic rats, PLoS ONE 7 (2012) e50402.
[23] M. Toporsian, R. Gros, M.G. Kabir, S. Vera, K. Govindaraju, D.H. Eidelman, M. Husain, M. Letarte, A role for endoglin in coupling eNOS activity and regulating vascular tone revealed in hereditary hemorrhagic telangiectasia, Circ. Res. 96 (2005) 684–692.
[24] C.M. Sena, A.M. Pereira, R. Seica, Endothelial dysfunction — a major mediator of diabetic vascular disease, Biochim. Biophys. Acta 1832 (2002) 2216–2231.
[25] S.M. Grundy, B. Howard, S. Smith Jr., R. Eckel, R. Redberg, R.O. Bonow, Prevention Conference VI: Diabetes and Cardiovascular Disease: executive summary: conference proceeding for healthcare professionals from a special writing group of the American Heart Association, Circulation 105 (2002) 2231–2239.
[26] T. Thum, D. Fraccarollo, M. Schultheiss, S. Froese, P. Galuppo, J.D. Widder, D. Tsikas, G. Ertl, J. Bauersachs, Endothelial nitric oxide synthase uncoupling impairs endothelial progenitor cell mobilization and function in diabetes, Diabetes 56 (2007) 666–674.
[27] S. Kumar, X. Sun, S. Wedgwood, S.M. Black, Hydrogen peroxide decreases endothelial nitric oxide synthase promoter activity through the inhibition of AP-1 activity, Am. J. Physiol. Lung Cell. Mol. Physiol. 295 (2008) L370–L377.

[28] J. Navarro-Antolin, J. Rey-Campos, S. Lamas, Transcriptional induction of endothelial nitric oxide gene by cyclosporine A. A role for activator protein-1, J. Biol. Chem. 275 (2000) 3075–3080.
[29] K.S. Lee, J. Kim, S.N. Kwak, K.S. Lee, D.K. Lee, K.S. Ha, M.H. Won, D. Jeoung, H. Lee, Y.G. Kwon, Y.M. Kim, Functional role of NF-κB in expression of human endothelial nitric oxide synthase, Biochem. Biophys. Res. Commun. 448 (2014) 101–107.
[30] V. Janssens, J. Goris, Protein phosphatase 2A: a highly regulated family of serine/threonine phosphatases implicated in cell growth and signaling, Biochem. J. 353 (2001) 417–439.
[31] I. Fleming, B. Fisslthaler, S. Dimmeler, B.E. Kemp, R. Busse, Phosphorylation of Thr(495) regulates Ca(2+)/calmodulin-dependent endothelial nitric oxide synthase activity, Circ. Res. 88 (2001) E68–E75.